EURASIAN BULLETIN OF MATHEMATICS
EBM (2018), VOL. 1, NO. 3, 94-97

The Generalized Odd Inverted Exponential-G family of Distributions: Properties and Applications

C. Chesneau[1,*], S. Djibrila[1]
LMNO, University of Caen-Normandie, Caen, 14032, France[1]

Abstract. In this article, we introduce a new family of distributions, called the generalized odd inverted exponential-G family. Its main feature is to use a new flexible generalization of the so-called odd transformation based on a weighting technique. We study some of its mathematical properties such that asymptotic, quantile function, linear representation, moments, reliability, entropy, order statistics and bivariate extension. Then, the inferential aspect of the corresponding statistical model is explored. The maximum likelihood estimation of the parameters is discussed and a Monte Carlo simulation study shows the good performances of the obtained estimates. The usefulness and flexibility of the new family of distributions is demonstrated through three practical data sets. It is shown that some generalized odd inverted exponential-G special models can outperform well-established models in the literature.
2010 Mathematics Subject Classifications: 60E05; 62E15; 62F10.
Key Words and Phrases: Inverted exponential distribution; odd transformation; maximum likelihood estimation; data analysis.

1. Introduction

Many fields such as biology, insurance, engineering, economics, environmental sciences, medicine, which are intended to be more productive and exigent, use statistics to understand, model and treat a wide variety of data. For this reason, they use standard probability distributions which, despite their high efficiency, present some limitations for specific data sets. As solutions, statisticians are extending these distributions by adding one or more parameters to obtain a high degree of flexibility. Among these generalizations, we can mention several families of distributions as the odd power Cauchy family by [1], the generalized odd log-logistic family by [11], the beta-G family by [13], the Kumaraswamy-G family by [2], the gamma-X family by [4], the gamma-G (type 1) family by [26], the gamma-G (type 2) family by [23], the gamma-G (type 3) family by [24], the log-gamma-G family [7], the logistic-G family by [25], the exponentiated generalized-G family by [12], the transformed-transformer family by [5] and the exponentiated T-X family by [6].

Recently, new families of distributions arise by the use of the so-called T-X transformation introduced by [5], defined with Fréchet distributions like and the so-called odd transformation defined by $\mathrm{odd}(u) = \frac{u}{1-u}$, $u \in (0,1)$. One of the most significant of them is the odd Fréchet-G family introduced by [15], characterized by the cumulative density function (cdf) given by

$$F(x;\lambda,\theta) = e^{-\left[\frac{1-G(x;\xi)}{G(x;\xi)}\right]^{\theta}}, \quad x \in \mathbb{R}, \tag{1.1}$$

*Corresponding author.

Email address: `salioubijou@gmail.com; christophe.chesneau@unicaen.fr* (Corresponding Author)`

where $\theta > 0$ and $G(x;\xi)$ is the cdf of a (generally well-known) continuous distribution, ξ denoting its parameters vector. More applications on the odd Fréchet-G family are given in [3]. Also, an extension of the odd Fréchet-G family is explored in [21]. These new families have the merits to deal with tractable functions, enjoy nice mathematical properties and allow the construction of very flexible statistical models. In the same purpose, we propose a new family of distributions called generalized odd inverted exponential-G (GOIE-G) family characterized by the cdf given by

$$F(x;\lambda,\gamma,\xi) = e^{-\frac{\lambda[1-G(x;\xi)][1+\gamma G(x;\xi)]}{G(x;\xi)}}, \quad x \in \mathbb{R}, \tag{1.2}$$

where $\lambda > 0$ and $\gamma \geq -1$. In the next, we denote this family by GOIE-G(λ,γ,ξ) and a random variable X having this cdf is denoted as $X \sim$ GOIE-G(λ,γ,ξ). Let us now motivate the interest of the GOIE-G family. The expression of $F(x;\lambda,\gamma,\xi)$ is based on the T-X transformation of the form

$$F(x;\lambda,\gamma,\xi) = \int_0^{W[G(x;\xi)]} r(t)dt,$$

where $r(t)$ denotes the probability density function (pdf) of the inverse exponential distribution, i.e., $r(t) = \frac{\lambda}{t^2}e^{-\frac{\lambda}{t}}$, $t > 0$, which can be viewed as simple special case of the Fréchet distribution (in a same spirit to [15], [3] and [21], among others), and $W(u) = \mathrm{odd}(u)w(u)$, $u \in (0,1)$, where

$$w(u) = \frac{1}{1+\gamma u}.$$

The main novelty in this construction is the use of $W(u)$, which provides a new extended odd transformation. Instead of considering an exponentiated version of odd(u) as in (1.1), we propose to weight it by $w(u)$, which is a simple weight function depending on a tuning parameter γ. The consideration of $W(u)$ is motivated by the following facts. First of all, $W(u)$ satisfies the standard conditions of those required by the T-X transformation, i.e.,

$$\begin{cases} W(u) \in (0,+\infty) \text{ (the support of the function } r(t)), \\ W(u) \text{ is differentiable and monotonically non-decreasing on } (0,1), \\ W(u) \to 0 \text{ as } u \to 0, \\ W(u) \to +\infty \text{ as } u \to 1. \end{cases}$$

Secondly, note that, if $\gamma = 0$, then $W(u) = \mathrm{odd}(u)$, if $\gamma > 0$, we have the following inequalities: $\mathrm{odd}(u) \geq W(u) \geq \frac{1}{1+\gamma}\,\mathrm{odd}(u)$ and, if $\gamma \in (-1,0)$, we have the reverse inequalities: $\mathrm{odd}(u) \leq W(u) \leq \frac{1}{1+\gamma}\,\mathrm{odd}(u)$. In this sense, the parameter γ has the ability to modulate the importance of odd(u) according to the context, opening new perspective of applications. Last but not least, $W(u)$ has a tractable expression with an explicit inverse function, i.e.,

$$W^{-1}(u) = \frac{(\gamma-1)u - 1 + \sqrt{[1-(\gamma-1)u]^2 + 4\gamma u^2}}{2\gamma u}, \quad u \in (0,1).$$

This allows to determine the analytical expressions of important incoming quantities related to the GOIE-G family (quantile function, kurtosis, skewness and so on). This point will be developed in detail later.

In order to better handle the GOIE-G family, let us now express the corresponding pdf and hazard rate function (hrf), playing a fundamental role in probability theory. By differentiating (1.2), the pdf of the GOIE-G family is given by

$$f(x;\lambda,\gamma,\xi) = \frac{\lambda[1+\gamma G(x;\xi)^2]g(x;\xi)}{G(x;\xi)^2} e^{-\frac{\lambda[1-G(x;\xi)][1+\gamma G(x;\xi)]}{G(x;\xi)}}, \quad x \in \mathbb{R}, \tag{1.3}$$

where $g(x;\xi)$ is the pdf corresponding to $G(x;\xi)$.

The corresponding hrf is given by

$$h(x;\lambda,\gamma,\xi) = \frac{f(x;\lambda,\gamma,\xi)}{1-F(x;\lambda,\gamma,\xi)} = \frac{\lambda[1+\gamma G(x;\xi)^2]g(x;\xi)}{\left(e^{\frac{\lambda[1-G(x;\xi)][1+\gamma G(x;\xi)]}{G(x;\xi)}}-1\right)G(x;\xi)^2}, \quad x\in\mathbb{R}. \tag{1.4}$$

The aim of this paper is to provide a detailed study of this new family, including a mathematical treatment of its main properties, statistical inference, with simulation and applications to several practical data sets, with discussions. In particular, we show that some generalized odd inverted exponential-G model can outperform well-established models in the literature, including some proposed in [21] and [22].

The paper is organized as follows. In Section 2, we give the expressions of the pdf, cdf and hrf of three special models based on the exponential, Weibull and Lindley distributions, with some representative plots. In Section 3, we provide the mathematical properties of the family such as asymptotic, shape of the crucial functions, quantile function, linear representation and so on. In Section 4, some inferential aspects of the GOIE-G family is explored. Section 5 is dedicated to applications to prove empirically the flexibility of the new model. Finally, some concluding remarks are addressed in Section 6.

2. Special distributions

In this section, we introduce three special distributions belonging to the GOIE-G family, namely:

- the generalized odd inverted exponential exponential (GOIE-E) distribution,
- the generalized odd inverted exponential Weibull (GOIE-W) distribution,
- the generalized odd inverted exponential Lindley (GOIE-L) distribution.

2.1. GOIE-E distribution

Let us consider the exponential distribution as baseline distribution, with the cdf given by $G(x;\theta)=1-e^{-\theta x}$ and the pdf given by $g(x;\theta)=\theta e^{-\theta x}$, $x>0$, $\theta>0$. Then, based on (1.2), the cdf of the GOIE-E distribution is given by

$$F(x;\lambda,\gamma,\theta) = e^{-\frac{\lambda[1+\gamma(1-e^{-\theta x})]}{e^{\theta x}-1}}, \quad x>0.$$

The corresponding pdf is defined by

$$f(x;\lambda,\gamma,\theta) = \frac{\theta\lambda[1+\gamma(1-e^{-\theta x})^2]}{(1-e^{-\theta x})^2} e^{-\frac{\lambda[1+\gamma(1-e^{-\theta x})]}{e^{\theta x}-1}-\theta x}, \quad x>0.$$

The corresponding hrf is given by

$$h(x;\lambda,\gamma,\lambda) = \frac{\theta\lambda[1+\gamma(1-e^{-\theta x})^2]e^{-\theta x}}{\left(e^{\frac{\lambda[1+\gamma(1-e^{-\theta x})]}{e^{\theta x}-1}}-1\right)(1-e^{-\theta x})^2}, \quad x>0.$$

Figure 1 shows plots of the pdf of the GOIE-E distribution, whereas Figure 2 shows plots of the corresponding hrf, for selected values of the parameters.

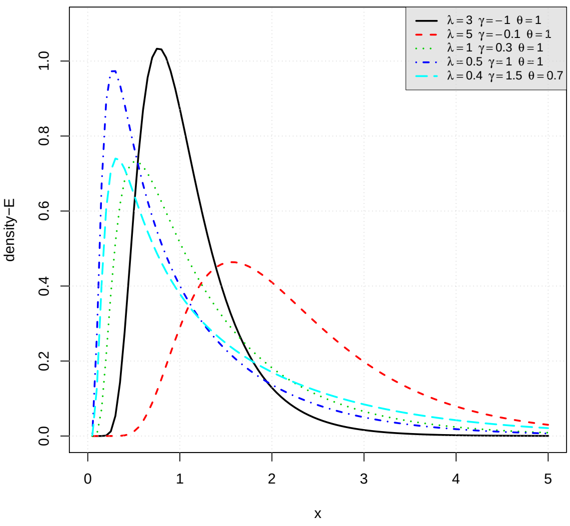

Figure 1: Plots of GOIE-E pdf.

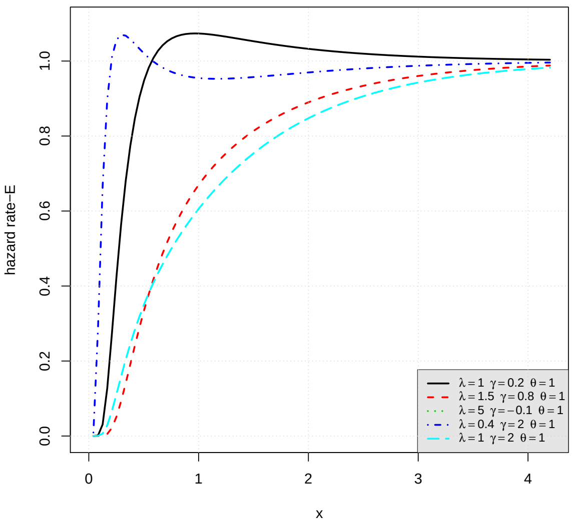

Figure 2: Plots of GOIE-E hrf.

2.2. GOIE-W distribution

Let us now consider the Weibull distribution as baseline distribution, with the cdf given by $G(x;a,b) = 1-e^{-(\frac{x}{b})^a}$ and the pdf given by $g(x;a,b) = \frac{a}{b}(\frac{x}{b})^{a-1}e^{-(\frac{x}{b})^a}$, $x>0$, $a>0$, $b>0$. Then, based on (1.2), the cdf of the GOIE-W distribution is given by

$$F(x;\lambda,\gamma,a,b) = e^{-\frac{\lambda[1+\gamma(1-e^{-(\frac{x}{b})^a})]}{e^{(\frac{x}{b})^a}-1}}, \quad x>0.$$

The corresponding pdf is defined by

$$f(x;\lambda,\gamma,a,b) = \frac{a\lambda x^{a-1}[1+\gamma(1-e^{-(\frac{x}{b})^a})^2]}{b^a(1-e^{-(\frac{x}{b})^a})^2} e^{-\frac{\lambda[1+\gamma(1-e^{-(\frac{x}{b})^a})]}{e^{(\frac{x}{b})^a}-1}-(\frac{x}{b})^a}, \quad x>0.$$

The corresponding hrf is given by

$$h(x;\lambda,\gamma,a,b) = \frac{a\lambda x^{a-1}[1+\gamma(1-e^{-(\frac{x}{b})^a})^2]e^{-(\frac{x}{b})^a}}{b^a(1-e^{-(\frac{x}{b})^a})^2\left(e^{\frac{\lambda[1+\gamma(1-e^{-(\frac{x}{b})^a})]}{e^{(\frac{x}{b})^a}-1}}-1\right)}, \quad x>0.$$

Figure 3 shows plots of the pdf of the GOIE-W distribution, whereas Figure 4 shows plots of the GOIE-W distribution.

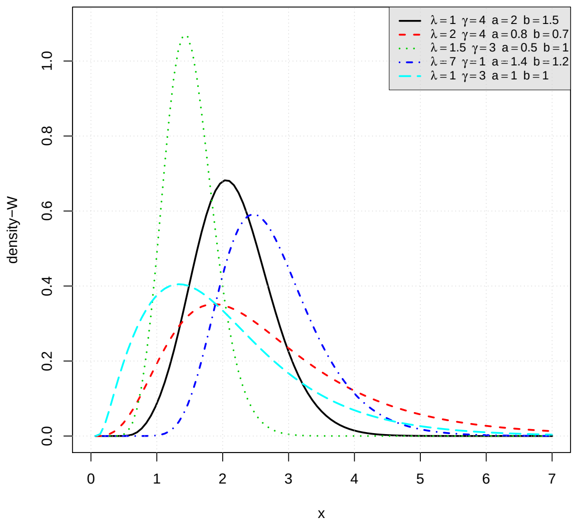

Figure 3: Plots of GOIE-W pdf.

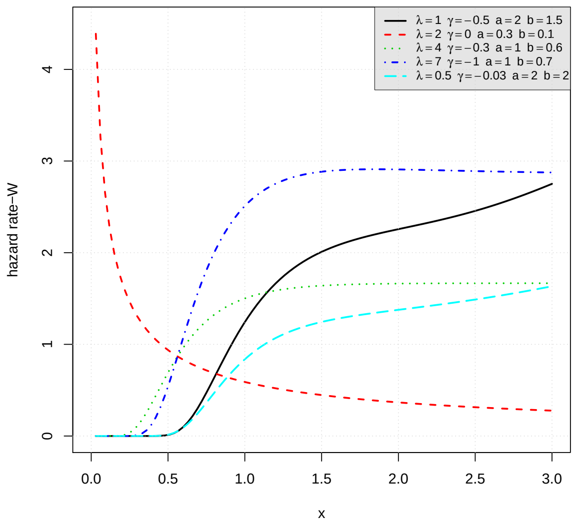

Figure 4: Plots of GOIE-W hrf.

2.3. GOIE-L distribution

Let us now consider the Lindley distribution as baseline distribution, with the cdf given by $G(x;\theta) = 1 - \frac{1+\theta+\theta x}{1+\theta} e^{-\theta x}$ and the pdf given by $g(x;\theta) = \frac{\theta^2}{1+\theta}(1+x)e^{-\theta x}$, $x > 0$, $\theta > 0$. Then, based on (1.2), the cdf of the GOIE-L distribution is given by

$$F(x;\lambda,\gamma,\theta) = e^{-\frac{\lambda(1+\theta+\theta x)[1+\gamma(1-\frac{1+\theta+\theta x}{1+\theta}e^{-\theta x})]e^{-\theta x}}{1+\theta-(1+\theta+\theta x)e^{-\theta x}}}, \quad x > 0.$$

The corresponding pdf is defined by

$$f(x;\lambda,\gamma,\theta) = \frac{\lambda\theta^2[1+\gamma(1-\frac{1+\theta+\theta x}{1+\theta}e^{-\theta x})^2](1+x)}{(1+\theta)(1-\frac{1+\theta+\theta x}{1+\theta}e^{-\theta x})^2} e^{-\frac{\lambda(1+\theta+\theta x)[1+\gamma(1-\frac{1+\theta+\theta x}{1+\theta}e^{-\theta x})]e^{-\theta x}}{1+\theta-(1+\theta+\theta x)e^{-\theta x}} - \theta x}, \quad x > 0.$$

The corresponding hrf is given by

$$h(x;\lambda,\gamma,\theta) = \frac{\lambda\theta^2[1+\gamma(1-\frac{1+\theta+\theta x}{1+\theta}e^{-\theta x})^2](1+x)e^{-\theta x}}{(1+\theta)(1-\frac{1+\theta+\theta x}{1+\theta}e^{-\theta x})^2\left(e^{\frac{\lambda(1+\theta+\theta x)[1+\gamma(1-\frac{1+\theta+\theta x}{1+\theta}e^{-\theta x})]e^{-\theta x}}{1+\theta-(1+\theta+\theta x)e^{-\theta x}}} - 1\right)}, \quad x > 0.$$

Figure 5 presents plots of the pdf of the GOIE-L distribution, whereas Figure 6 shows plots of the hrf of the GOIE-L distribution.

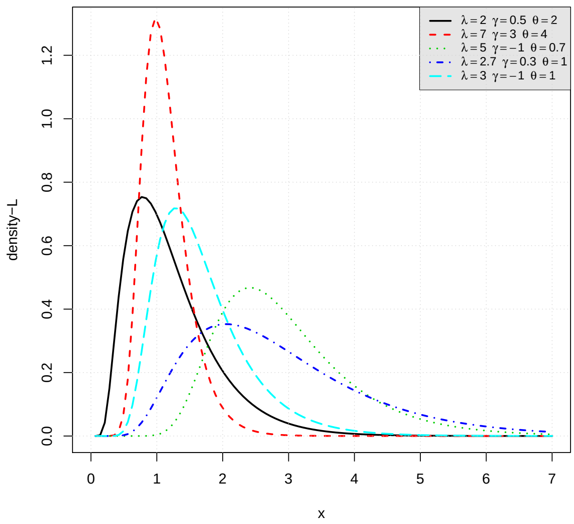

Figure 5: Plots of GOIE-L pdf.

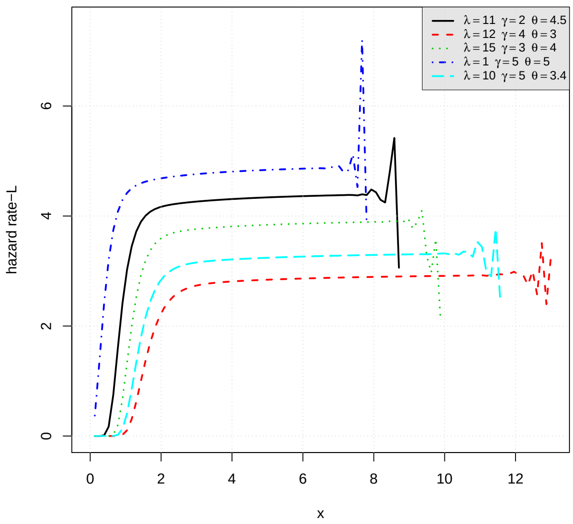

Figure 6: Plots of GOIE-L hrf.

In Figures 1, 3 and 5, all the presented pdfs are unimodal and mainly right skewed with different degrees of heaviness. In Figures 2, 4 and 6, various kinds of shapes for the hrfs are observed, simple or complex. Thus, through these visualized graphs, we can expect a great flexibility of the GOIE-G family for modelling right skewed, left skewed and symmetric data.

3. Mathematics properties

This section is devoted to the mathematical properties of the GOIE-G family. Let us recall that it is characterized by the cdf $F(x;\lambda,\gamma,\xi)$ given by (1.2), with pdf $f(x;\lambda,\gamma,\xi)$ given by (1.3) and hrf $h(x;\lambda,\gamma,\xi)$ given by (1.4). We focus on some basic results in distribution, the asymptotic of the main functions, the critical points of the crucial functions, the quantile function, some linear representations, the moments, the reliability, the entropy, the order statistics and a bivariate extension.

3.1. Basic results in distribution

Here, some basic results in distribution involving the GOIE-G family are presented. Let $X \sim$ GOIE-G(λ,γ,ξ). If we set $Y = G(X;\xi)$, then the cdf of Y is given by: $F_Y(y) = e^{-\frac{\lambda(1-y)(1+\gamma y)}{y}}$, $y \in (0,1)$. To the best of our knowledge, $F_Y(y)$ is not a listed cdf in the literature (excepted for the special case $\gamma = 0$). Furthermore, if we set $Z = \frac{G(X;\xi)}{[1-G(X;\xi)][1+\gamma G(X;\xi)]}$, then Z follows the inverted exponential distribution.

3.2. Asymptotic

The main asymptotic properties of $F(x;\lambda,\gamma,\xi)$, $f(x;\lambda,\gamma,\xi)$ and $h(x;\lambda,\gamma,\xi)$ are investigated below. Let $\delta = \inf\{x \in \mathbb{R};\ G(x;\xi) > 0\}$ and $\beta = e^{\lambda(1-\gamma)}$. When $x \to \delta$, we have

$$F(x;\lambda,\gamma,\xi) \sim \beta e^{-\frac{\lambda}{G(x;\xi)}}, \quad f(x;\lambda,\gamma,\xi) \sim \beta\lambda \frac{g(x;\xi)}{G(x;\xi)^2} e^{-\frac{\lambda}{G(x;\xi)}}, \quad h(x;\lambda,\gamma,\xi) \sim \beta\lambda \frac{g(x;\xi)}{G(x;\xi)^2} e^{-\frac{\lambda}{G(x;\xi)}}.$$

When $x \to +\infty$, we have

$$F(x;\lambda,\gamma,\xi) - 1 \sim -\lambda(1+\gamma)[1-G(x;\xi)], \quad f(x;\lambda,\gamma,\xi) \sim \lambda(1+\gamma)g(x;\xi), \quad h(x;\lambda,\gamma,\xi) \sim \frac{g(x;\xi)}{1-G(x;\xi)}.$$

We thus see the impact of the parameters λ and γ in the asymptotes of these functions.

3.3. Critical points of the crucial functions

The shapes of the pdf and the hrf of the GOIE-G family can be described analytically. The critical points of $f(x;\lambda,\gamma,\xi)$ are the roots of the following equation: $f'(x;\lambda,\gamma,\xi) = 0$, which can be reduced to

$$\frac{1+\gamma G(x;\xi)^2}{G(x;\xi)^2} g'(x;\xi) - \frac{2g(x;\xi)^2}{G(x;\xi)^3} + \frac{\lambda[1+\gamma G(x;\xi)^2]^2 g(x;\xi)^2}{G(x;\xi)^4} = 0. \tag{3.1}$$

The critical points of $h(x;\lambda,\gamma,\xi)$ are obtained from the following equation: $h'(x;\lambda,\gamma,\xi) = 0$, which can be reduced to

$$\frac{1+\gamma G(x;\xi)^2}{G(x;\xi)^2} g'(x;\xi) - \frac{2g(x;\xi)^2}{G(x;\xi)^3} + \frac{\lambda[1+\gamma G(x;\xi)^2]^2 g(x;\xi)^2}{\left(1 - e^{-\frac{\lambda[1-G(x;\xi)][1+\gamma G(x;\xi)]}{G(x;\xi)}}\right) G(x;\xi)^4} = 0. \tag{3.2}$$

There may be more than one root to (3.1) and (3.2). By using most of the symbolic computation software platforms, we can determine these roots, as well as their nature (local maximums and minimums and inflection points).

3.4. Quantile function, skewness and kurtosis

Let $Q_G(x;\xi)$ be the quantile function (qf) corresponding to $G(x;\xi)$. Then, the qf of the GOIE-G family is given by

- for $\gamma = 0$,

$$Q(u;\lambda,\gamma,\xi) = Q_G\left(\frac{\lambda}{\lambda - \log(u)};\xi\right),$$

- for $\gamma \neq 0$,

$$Q(u;\lambda,\gamma,\xi) = Q_G\left(\frac{\log(u) + \lambda(\gamma-1) + \sqrt{[\log(u)+\lambda(\gamma-1)]^2 + 4\lambda^2\gamma}}{2\lambda\gamma};\xi\right),$$

  $u \in (0,1)$.

As usual, important quantiles can be obtained with particular values for u, as the median given by $M = Q(0.5; \lambda, \gamma, \xi)$. One can also use the quantile function for simulation purposes. Indeed, if U is a random variable following the uniform distribution over $(0, 1)$, then $X = Q(U; \lambda, \gamma, \xi)$ has the cdf given by (1.2).

On the other side, in full generality, the effects of the shape parameters on the skewness and kurtosis of a distribution can be evaluated via qf measures. For instance, we can use the Bowley skewness given by

$$Sk = \frac{Q(\frac{1}{4}; \lambda, \gamma, \xi) + Q(\frac{3}{4}; \lambda, \gamma, \xi) - 2Q(\frac{1}{2}; \lambda, \gamma, \xi)}{Q(\frac{3}{4}; \lambda, \gamma, \xi) - Q(\frac{1}{4}; \lambda, \gamma, \xi)},$$

and the Moors kurtosis given by

$$Kt = \frac{Q(\frac{7}{8}; \lambda, \gamma, \xi) - Q(\frac{5}{8}; \lambda, \gamma, \xi) + Q(\frac{3}{8}; \lambda, \gamma, \xi) - Q(\frac{1}{8}; \lambda, \gamma, \xi)}{Q(\frac{6}{8}; \lambda, \gamma, \xi) - Q(\frac{2}{8}; \lambda, \gamma, \xi)}.$$

We refer to [19] and [14] for further details on these measures.

As illustrations, the plots of the Bowley skewness and Moors kurtosis of the GOIE-W distribution presented in Subsection 2.2 are displayed in Figures 7 and 8, respectively. For each case, when γ increases and λ fixed, skewness and kurtosis decrease. Moreover, there exists λ_* such that, when $\lambda \leq \lambda_*$ and γ fixed, skewness and kurtosis increase and for $\lambda \geq \lambda_*$ decrease. Thus, the impact of the values of γ and λ on the skewness and kurtosis is significant.

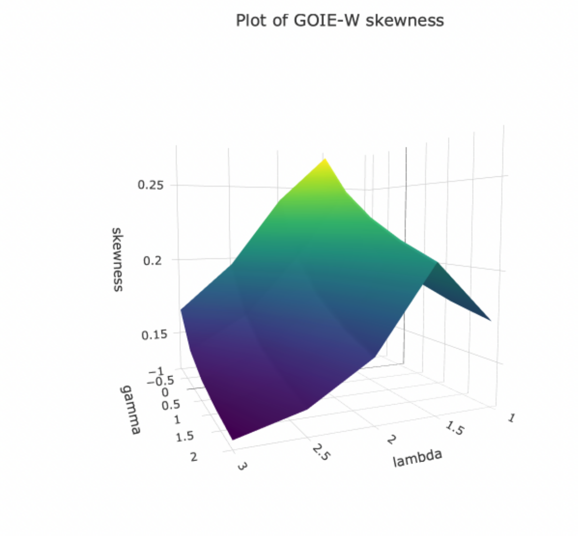

Figure 7: Plot of GOIE-W skewness.

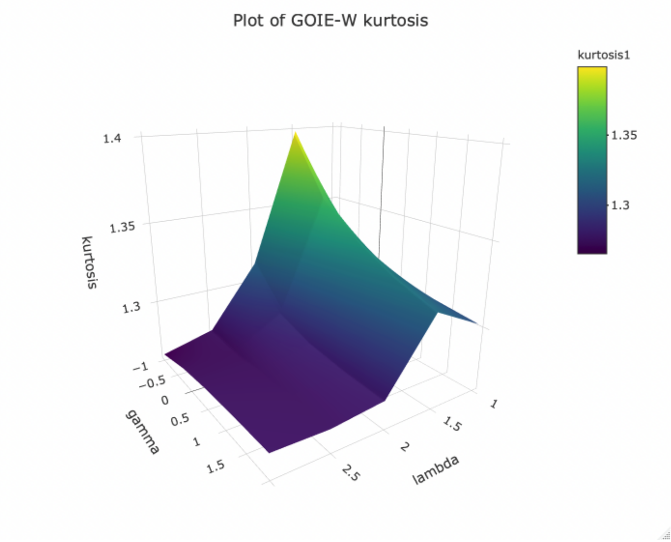

Figure 8: Plot of GOIE-W kurtosis.

3.5. Linear representation

In this subsection, we give the linear representations of the pdf and cdf of the GOIE-G family in terms of exp-G distribution of the baseline distribution, which will be useful for the derivation of further properties.

Proposition 3.1. *A linear representation of the cdf of the GOIE-G family is given by*

$$F(x; \lambda, \gamma, \xi) = \sum_{k,\ell=0}^{+\infty} \sum_{i=0}^{k+\ell} \sum_{j=0}^{k} m_{ijk\ell} G(x; \xi)^{i+j}, \tag{3.3}$$

where $m_{ijk\ell} = \frac{(-1)^{i+k+\ell}\lambda^k\gamma^j}{k!}\binom{-k}{\ell}\binom{k+\ell}{i}\binom{k}{j}$.

Proof. By using the series expansion of the exponential function, we get

$$F(x;\lambda,\gamma,\xi) = \sum_{k=0}^{+\infty}\frac{(-\lambda)^k}{k!}\frac{[1-G(x;\xi)]^k[1+\gamma G(x;\xi)]^k}{G(x;\xi)^k}.$$

On the other side, the general binomial formula gives

$$\frac{1}{G(x;\xi)^k} = (1-[1-G(x;\xi)])^{-k} = \sum_{\ell=0}^{+\infty}(-1)^\ell\binom{-k}{\ell}[1-G(x;\xi)]^\ell,$$

and the standard binomial formula gives

$$[1+\gamma G(x;\xi)]^k = \sum_{j=0}^{k}\gamma^j\binom{k}{j}G(x;\xi)^j$$

and

$$[1-G(x;\xi)]^{k+\ell} = \sum_{i=0}^{k+\ell}(-1)^i\binom{k+\ell}{i}G(x;\xi)^i.$$

Therefore,

$$\frac{[1-G(x;\xi)]^k[1+\gamma G(x;\xi)]^k}{G(x;\xi)^k} = \sum_{\ell=0}^{+\infty}\sum_{i=0}^{k+\ell}\sum_{j=0}^{k}(-1)^{i+\ell}\gamma^j\binom{-k}{\ell}\binom{k+\ell}{i}\binom{k}{j}G(x;\xi)^{i+j}.$$

By combining the equalities above, we obtain the desired linear representation. This ends the proof of Proposition 3.1. □

Corollary 3.2. *By differentiation of* (3.3)*, we have the following linear representation for the pdf of the GOIE-G family:*

$$f(x;\lambda,\gamma,\xi) = \sum_{k,\ell=0}^{+\infty}\sum_{i=0}^{k+\ell}\sum_{j=0,j>-i}^{k}(i+j)m_{ijk\ell}\,g(x;\xi)G(x;\xi)^{i+j-1}. \tag{3.4}$$

Let us note that, for the sake of correctness in the following developments, since the term corresponding to $i=0$ and $j=0$ in the sum is equal to 0, we have removed it (by adding the condition $j>-i$, i.e., $i+j\geq 1$). The linear representation (3.4) will be useful to simply express central probabilities measure. From a practical point of view, we can substitute $+\infty$ in the sums by a large positive integer such as 25 or 30 without a significant loss of precision. In what follows, we suppose that all the introduced integral terms exist and that exchange between sum and integral are possible (the Lebesgue theorem is applicable).

3.6. Moments

In this subsection, we give the explicit expression for the rth moment, the rth incomplete moment and the mean deviation. Let $X \sim$ GOIE-G. By using Corollary 3.2, the rth moment of X is given by

$$E(X^r) = \int_{-\infty}^{+\infty}x^r f(x;\lambda,\gamma,\xi)dx = \sum_{k,\ell=0}^{+\infty}\sum_{i=0}^{k+\ell}\sum_{j=0,j>-i}^{k}(i+j)m_{ijk\ell}\tau_{ij}(r),$$

where $\tau_{ij}(r) = \int_{-\infty}^{+\infty} x^r g(x;\xi)G(x;\xi)^{i+j-1}dx = \int_0^1 Q_G(u;\xi)^r u^{i+j-1}du$. For a given $G(x;\xi)$, the integral term can be evaluated as least numerically. As usual, the mean of X is given by $\mu = E(X)$ and the variance of X is given by $V(X) = E(X^2) - [E(X)]^2$.

For empirical reasons, the nature of many distributions may usefully be described by what we call incomplete moments. For $y \in \mathbb{R}$, the rth incomplete moment of X can be determined as

$$m_r(y) = \int_{-\infty}^{y} x^r f(x;\lambda,\gamma,\xi)dx = \sum_{k,\ell=0}^{+\infty}\sum_{i=0}^{k+\ell}\sum_{j=0,j>-i}^{k}(i+j)m_{ijk\ell}\tau_{ij}^*(r,y),$$

where $\tau_{ij}^*(r,y) = \int_{-\infty}^{y} x^r g(x;\xi)G(x;\xi)^{i+j-1}dx = \int_0^{G(y;\xi)} Q_G(u;\xi)^r u^{i+j-1}du$. Finally, the mean deviation about the mean of X is given by

$$D(X) = 2[\mu F(\mu;\lambda,\gamma,\xi) - m_1(\mu)].$$

As illustration, Table 1 indicates some numerical results on the moments, variances and means deviation of the GOIE-W distribution presented in Subsection 2.2, for selected values of the parameters.

Table 1: Moments, variances and mean deviations of the GOIE-W distribution for some parameter values of a and b for fixed values $\lambda = 1.5$ and $\gamma = 1$.

	$a=2,b=1.5$	$a=0.8,b=0.7$	$a=2,b=1$	$a=1.4,b=1.2$	$a=1,b=2$
$E(X)$	1.953009	1.594979	1.302006	1.798269	1.852098
$E(X^2)$	4.16722	4.144662	1.852098	3.850388	4.752611
$E(X^3)$	9.646906	15.91562	2.858342	9.618552	16.01992
$E(X^4)$	24.06009	83.89284	4.752611	27.51172	67.87932
$V(X)$	0.352975	1.600704	0.1568784	0.6166166	1.322344
$D(X)$	0.474128	0.920521	0.3160853	0.6158726	1.742454

In a similar way, we can express the moment generating function of X as

$$M(t) = E(e^{tX}) = \int_{-\infty}^{+\infty} e^{tx} f(x;\lambda,\gamma,\xi)dx = \sum_{k,\ell=0}^{+\infty}\sum_{i=0}^{k+\ell}\sum_{j=0,j>-i}^{k}(i+j)m_{ijk\ell}\zeta_{ij}(t),$$

where $\zeta_{ij}(t) = \int_{-\infty}^{+\infty} e^{tx} g(x;\xi)G(x;\xi)^{i+j-1}dx = \int_0^1 e^{tQ_G(u;\xi)} u^{i+j-1}du$.

3.7. Reliability parameter

In the GOIE-G family context, we consider the following reliability scenario. The stress strength model defines the lifetime of an element that has a random strength, modeled by $X_1 \sim$ GOIE-G$(\lambda_1,\gamma_1,\xi_1)$, that is exposed to an accidental stress, modeled by $X_2 \sim$ GOIE-G$(\lambda_2,\gamma_2,\xi_2)$. The device breaks down when the stress applied to it exceeds the strength, and the device will be working properly each time $X_1 > X_2$. Thus, the probability $R = P(X_1 > X_2)$ is a measure of reliability. It has many applications, particularly in the field of reliability and engineering (see [17], for instance). Here, we derive the reliability parameter R when X_1 and X_2 are independent. Let us denote by $f(x;\lambda_1,\gamma_1,\xi_1)$ the pdf of X_1 and $F(x;\lambda_2,\gamma_2,\xi_2)$ the cdf of X_2. Then, we have

$$R = \int_{-\infty}^{+\infty} f(x;\lambda_1,\gamma_1,\xi_1)F(x;\lambda_2,\gamma_2,\xi_2)dx.$$

Then, by applying Proposition 3.1 and Corollary 3.2, we have the following linear representations:

$$F(x;\lambda_2,\gamma_2,\xi_2)=\sum_{k,\ell=0}^{+\infty}\sum_{i=0}^{k+\ell}\sum_{j=0}^{k} m_{ijk\ell}G(x;\xi_2)^{i+j},$$

with $m_{ijk\ell}=\frac{(-1)^{i+k+\ell}\lambda_2^k\gamma_2^j}{k!}\binom{-k}{\ell}\binom{k+\ell}{i}\binom{k}{j}$ and

$$f(x;\lambda_1,\gamma_1,\xi_1)=\sum_{s,t=0}^{+\infty}\sum_{q=0}^{s+t}\sum_{r=0,r>-q}^{s}(q+r)m^*_{qrst}g(x;\xi_1)G(x;\xi_1)^{q+r-1},$$

with $m^*_{qrst}=\frac{(-1)^{q+s+t}\lambda_1^s\gamma_1^r}{s!}\binom{-s}{t}\binom{s+t}{q}\binom{s}{r}$.

Hence, we can be express R as

$$R=\sum_{k,\ell,s,t=0}^{+\infty}\sum_{i=0}^{k+\ell}\sum_{j=0}^{k}\sum_{q=0}^{s+t}\sum_{r=0,r>-q}^{s}(q+r)m_{ijk\ell}m^*_{qrst}\int_{-\infty}^{+\infty}g(x;\xi_1)G(x;\xi_1)^{q+r-1}G(x;\xi_2)^{i+j}dx.$$

For a given $G(x;\xi)$, the integral term can be evaluated numerically. In the cases of $\lambda_1=\lambda_2$, $\gamma_1=\gamma_2$ and $\xi_1=\xi_2$, X_1 and X_2 are identically distributed, implying that $R=\frac{1}{2}$.

3.8. Entropy

Let $X\sim$ GOIE-G and $\alpha>0$ with $\alpha\neq 1$. Then, the Rényi entropy of X is given by

$$H_\alpha(X)=\frac{1}{1-\alpha}\log\left\{\int_{-\infty}^{+\infty}f(x;\lambda,\gamma,\xi)^\alpha dx\right\}.$$

In order to give a tractable expression for $H_\alpha(X)$, the result below investigates a linear representation for $f(x;\lambda,\gamma,\xi)^\alpha$.

Proposition 3.3. *We have the following linear representation for $f(x;\lambda,\gamma,\xi)^\alpha$:*

$$f(x;\lambda,\gamma,\xi)^\alpha=\sum_{k,\ell,q,s=0}^{+\infty}\sum_{i=0}^{k+\ell}\sum_{j=0}^{k}\sum_{r=0}^{q}\sum_{t=0}^{s}\rho_{ijk\ell qrst}g(x;\xi)^\alpha G(x;\xi)^{2r+t+i+j},$$

where

$$\rho_{ijk\ell qrst}=\frac{(-1)^{i+k+\ell+q+r+s+t}\lambda^{k+\alpha}\alpha^k\gamma^{j+q}}{k!(1+\gamma)^{q-\alpha}}\binom{-k}{\ell}\binom{k+\ell}{i}\binom{k}{j}\binom{\alpha}{q}\binom{q}{r}\binom{-2\alpha}{s}\binom{s}{t}.$$

Proof. We have

$$f(x;\lambda,\gamma,\xi)^\alpha=\frac{\lambda^\alpha g(x;\xi)^\alpha[1+\gamma G(x;\xi)^2]^\alpha}{G(x;\xi)^{2\alpha}}F(x;\lambda,\gamma,\xi)^\alpha.$$

By using the generalized binomial formula, we have

$$[1+\gamma G(x;\xi)^2]^\alpha=(1+\gamma)^\alpha\left(1-\frac{\gamma}{1+\gamma}[1-G(x;\xi)^2]\right)^\alpha$$

$$= \sum_{q=0}^{+\infty} \sum_{r=0}^{q} (-1)^{q+r} \frac{\gamma^q}{(1+\gamma)^{q-\alpha}} \binom{\alpha}{q} \binom{q}{r} G(x;\xi)^{2r}$$

and

$$\frac{1}{G(x;\xi)^{2\alpha}} = (1 - [1 - G(x;\xi)])^{-2\alpha} = \sum_{s=0}^{+\infty} \sum_{t=0}^{s} (-1)^{s+t} \binom{-2\alpha}{s} \binom{s}{t} G(x;\xi)^t.$$

On the other side, by proceeding as in the proof of Proposition 3.1, we have

$$F(x;\lambda,\gamma,\xi)^\alpha = \sum_{k,\ell=0}^{+\infty} \sum_{i=0}^{k+\ell} \sum_{j=0}^{k} \frac{(-1)^{i+k+\ell} \lambda^k \alpha^k \gamma^j}{k!} \binom{-k}{\ell} \binom{k+\ell}{i} \binom{k}{j} G(x;\xi)^{i+j}.$$

By combining the equalities above, we obtain the desired linear representation. This ends the proof of Proposition 3.3. □

By applying Proposition 3.3, we obtain

$$H_\alpha(X) = \frac{1}{1-\alpha} \log \left\{ \sum_{k,\ell,q,s=0}^{+\infty} \sum_{i=0}^{k+\ell} \sum_{j=0}^{k} \sum_{r=0}^{q} \sum_{t=0}^{s} \rho_{ijk\ell qrst} \int_{-\infty}^{+\infty} g(x;\xi)^\alpha G(x;\xi)^{2r+t+i+j} dx \right\}. \quad (3.5)$$

It also exists other measures of entropy such that Shannon entropy, Hartley entropy, entropy of collision, min entropy and so on, which are particular cases of Rényi entropy. In particular, we obtain Shannon entropy as $S(X) = \lim_{\alpha \to 1} H_\alpha(X)$.

3.9. Order statistics

Let $X \sim$ GOIE-G, $X_1, \ldots, X_n$ be a random sample from X and $X_{m:n}$ be the mth order statistic from $X_1, \ldots, X_n$. Then, the pdf of $X_{m:n}$ is given by

$$f_{m:n}(x;\lambda,\gamma,\xi) = \frac{n!}{(m-1)!(n-m)!} F(x;\lambda,\gamma,\xi)^{m-1} [1 - F(x;\lambda,\gamma,\xi)]^{n-m} f(x;\lambda,\gamma,\xi).$$

Using the binomial formula, we have

$$f_{m:n}(x;\lambda,\gamma,\xi) = \frac{n!}{(m-1)!(n-m)!} \sum_{d=0}^{n-m} (-1)^d \binom{n-m}{d} f(x;\lambda,\gamma,\xi) F(x;\lambda,\gamma,\xi)^{d+m-1}.$$

Following the steps of the proof of Proposition 3.1, we show that

$$F(x;\lambda,\gamma,\xi)^{d+m-1} = \sum_{k,\ell=0}^{+\infty} \sum_{i=0}^{k+\ell} \sum_{j=0}^{k} \frac{(-1)^{i+k+\ell} \lambda^k (d+m-1)^k \gamma^j}{k!} \binom{-k}{\ell} \binom{k+\ell}{i} \binom{k}{j} G(x;\xi)^{i+j}.$$

From Corollary 3.2 and the above equation, we obtain a linear expression of $f_{m:n}(x;\lambda,\gamma,\xi)$ in terms of pdfs of the exp-G family. Thus, several mathematical quantities of these order statistics like ordinary and incomplete moments, mgf, mean deviations and several others can be determined from those quantities of the exp-G distribution.

3.10. Bivariate extension

We now propose a bivariate version of the GOIE-G family, which can be useful to model bivariate data. It is called the bivariate odd generalized inverted exponential (BIGOIE-G) family. We say that a couple of random variables (X, Y) belongs to the BIGOIE-G family if it has the cdf given by

$$F_{X,Y}(x, y; \lambda, \gamma, \xi) = e^{-\frac{\lambda[1-G(x,y;\xi)][1+\gamma G(x,y;\xi)]}{G(x,y;\xi)}}, \quad (x, y) \in \mathbb{R}^2,$$

where $G(x, y; \xi)$ is an absolutely bivariate continuous distribution with marginal cdfs given by $G_1(x; \xi)$ and $G_2(y; \xi)$. Then, the marginal cdfs are given by

$$F_X(x; \lambda, \gamma, \xi) = e^{-\frac{\lambda[1-G_1(x;\xi)][1+\gamma G_1(x;\xi)]}{G_1(x;\xi)}}, \quad x \in \mathbb{R}$$

and

$$F_Y(y; \lambda, \gamma, \xi) = e^{-\frac{\lambda[1-G_2(y;\xi)][1+\gamma G_2(y;\xi)]}{G_2(y;\xi)}}, \quad y \in \mathbb{R}.$$

The joint pdf of (X, Y) is given by $f_{X,Y}(x, y; \lambda, \gamma, \xi) = \frac{\partial^2 F_{X,Y}(x,y;\lambda,\gamma,\xi)}{\partial x \partial y}$, i.e., after some algebra,

$$f_{X,Y}(x, y; \lambda, \gamma, \xi) = \frac{\lambda[1 + \gamma G(x, y; \xi)^2]A(x, y; \lambda, \gamma, \xi)}{G(x, y; \xi)^2} e^{-\frac{\lambda[1-G(x,y;\xi)][1+\gamma G(x,y;\xi)]}{G(x,y;\xi)}}, \quad (x, y) \in \mathbb{R}^2,$$

where

$$\begin{aligned} A(x, y; \lambda, \gamma, \xi) = {} & \frac{\partial^2 G(x, y; \xi)}{\partial x \partial y} \\ & + \frac{\partial G(x, y; \xi)}{\partial x} \frac{\partial G(x, y; \xi)}{\partial y} \left(\frac{\lambda[1 + \gamma G(x, y; \xi)^2]}{G(x, y; \xi)^2} - \frac{2}{[1 + \gamma G(x, y; \xi)^2]G(x, y; \xi)} \right). \end{aligned}$$

The marginal pdfs are given by

$$f_X(x; \lambda, \gamma, \xi) = \frac{\lambda[1 + \gamma G_1(x; \xi)^2]g_1(x; \xi)}{G_1(x; \xi)^2} e^{-\frac{\lambda[1-G_1(x;\xi)][1+\gamma G_1(x;\xi)]}{G_1(x;\xi)}}$$

and

$$f_Y(y; \lambda, \gamma, \xi) = \frac{\lambda[1 + \gamma G_2(y; \xi)^2]g_2(y; \xi)}{G_2(y; \xi)^2} e^{-\frac{\lambda[1-G_2(y;\xi)][1+\gamma G_2(y;\xi)]}{G_2(y;\xi)}}.$$

The conditional pdfs are given by

$$f_{X|Y}(x|y; \lambda, \gamma, \xi) = \frac{[1 + \gamma G(x, y; \xi)^2]G_2(y; \xi)^2 A(x, y; \lambda, \gamma, \xi)}{[1 + \gamma G_2(y; \xi)^2]g_2(y; \xi)G(x, y; \xi)^2} e^{\frac{\lambda[1-G_2(y;\xi)][1+\gamma G_2(y;\xi)]}{G_2(y;\xi)} - \frac{\lambda[1-G(x,y;\xi)][1+\gamma G(x,y;\xi)]}{G(x,y;\xi)}}$$

and

$$f_{Y|X}(y|x; \lambda, \gamma, \xi) = \frac{[1 + \gamma G(x, y; \xi)^2]G_1(x; \xi)^2 A(x, y; \lambda, \gamma, \xi)}{[1 + \gamma G_1(x; \xi)^2]g_1(x; \xi)G(x, y; \xi)^2} e^{\frac{\lambda[1-G_1(x;\xi)][1+\gamma G_1(x;\xi)]}{G_1(x;\xi)} - \frac{\lambda[1-G(x,y;\xi)][1+\gamma G(x,y;\xi)]}{G(x,y;\xi)}}.$$

From these expressions, moments or conditional moments can be expressed under the integral form.

4. Inferential consideration

In this section, some inferential aspects of the GOIE-G family are explored.

4.1. Maximum likelihood estimation

Here, we determine the maximum likelihood estimators (MLEs) of the model parameters of the new family from complete samples only. Let $x_1, \ldots, x_n$ be observations from the GOIE-G family with parameters λ, γ and ξ. We set $\Theta = (\lambda, \gamma, \xi)$, the parameter vector of interest, and we denote by r the number of parameters in the vector ξ. Then, the likelihood function is given by

$$L_n(\Theta) = \prod_{i=1}^{n} f(x_i;\Theta) = \lambda^n \left(\prod_{i=1}^{n} \frac{g(x_i;\xi)[1+\gamma G(x_i;\xi)^2]}{G(x_i;\xi)^2} \right) e^{-\lambda \sum_{i=1}^{n} \frac{[1-G(x_i;\xi)][1+\gamma G(x_i;\xi)]}{G(x_i;\xi)}}$$

The log-likelihood function is given by $\ell_n = \ell_n(\Theta) = \log L_n(\Theta)$, so

$$\ell_n = n\log(\lambda) + \sum_{i=1}^{n} \left(\log[g(x_i;\xi)] + \log[1+\gamma G(x_i;\xi)^2] - 2\log[G(x_i;\xi)] - \frac{\lambda[1-G(x_i;\xi)][1+\gamma G(x_i;\xi)]}{G(x_i;\xi)} \right).$$

If the first partial derivatives of ℓ_n exist, the MLEs of λ, γ and ξ can be obtained by solving the following equations: $\frac{\partial \ell_n}{\partial \lambda} = 0$, $\frac{\partial \ell_n}{\partial \gamma} = 0$, $\frac{\partial \ell_n}{\partial \xi_1} = 0$, $\ldots$, $\frac{\partial \ell_n}{\partial \xi_r} = 0$, simultaneously, according to λ, γ and ξ, where

$$\frac{\partial \ell_n}{\partial \lambda} = \frac{n}{\lambda} - \sum_{i=1}^{n} \frac{[1-G(x_i;\xi)][1+\gamma G(x_i;\xi)]}{G(x_i;\xi)},$$

$$\frac{\partial \ell_n}{\partial \gamma} = \sum_{i=1}^{n} \left(\frac{G(x_i;\xi)^2}{1+\gamma G(x_i;\xi)} - \lambda[1-G(x_i;\xi)] \right)$$

and, for $j = 1, \ldots, r$,

$$\frac{\partial \ell_n}{\partial \xi_j} = \sum_{i=1}^{n} \left(\frac{\partial g(x_i;\xi)}{\partial \xi_j} \frac{1}{g(x_i;\xi)} + \frac{\partial G(x_i;\xi)}{\partial \xi_j} \left\{ -\frac{2}{[1+\gamma G(x_i;\xi)^2]G(x;\xi)} + \frac{\lambda[1+\gamma G(x_i;\xi)^2]}{G(x_i;\xi)^2} \right\} \right).$$

The MLEs of λ, γ and ξ are denoted by $\hat{\lambda}$, $\hat{\gamma}$ and $\hat{\xi}$ and we set $\hat{\Theta} = (\hat{\lambda}, \hat{\gamma}, \hat{\xi})$. The corresponding observed information matrix at Θ_* is given by

$$J(\Theta_*) = - \left. \begin{pmatrix} \frac{\partial^2 \ell_n}{\partial \lambda^2} & \frac{\partial^2 \ell_n}{\partial \lambda \partial \gamma} & \frac{\partial^2 \ell_n}{\partial \lambda \partial \xi_1} & \cdots & \frac{\partial^2 \ell_n}{\partial \lambda \partial \xi_r} \\ . & \frac{\partial^2 \ell_n}{\partial \gamma^2} & \frac{\partial^2 \ell_n}{\partial \gamma \partial \xi_1} & \cdots & \frac{\partial^2 \ell_n}{\partial \gamma \partial \xi_r} \\ . & . & \frac{\partial^2 \ell_n}{\partial \xi_1^2} & \cdots & \frac{\partial^2 \ell_n}{\partial \xi_1 \partial \xi_r} \\ . & . & . & \cdots & . \\ . & . & . & \cdots & . \\ . & . & . & \cdots & \frac{\partial^2 \ell_n}{\partial \xi_r^2} \end{pmatrix} \right|_{\Theta = \Theta_*}.$$

Under some standard conditions of regularity, when $n \to +\infty$, the distribution of $\hat{\Theta}$ can be approximated by a multivariate normal distribution $\mathcal{N}_{r+2}(\Theta, J(\hat{\Theta})^{-1})$, where $J(\hat{\Theta})$ is the observed information matrix computed at $\hat{\Theta}$. Confidence intervals for the model parameters can be constructed from this result. Furthermore, the likelihood ratio (LR) test can be used for comparing the GOIE-G family with some of its special models. In particular, the LR test can be performed to check if the impact of the parameter γ is significant or not by considering the following hypotheses: $H_0 : \gamma = 0$ against $H_1 : \gamma \neq 0$. Thus, we compute the maximum values of the unrestricted and restricted log likelihood to construct the corresponding LR statistic. More precisely, it is reduced to $w = 2\left\{\ell(\hat{\lambda}, \hat{\gamma}, \hat{\xi}) - \ell(\tilde{\lambda}, 0, \tilde{\xi})\right\}$, where $\hat{\lambda}, \hat{\gamma}$ and $\hat{\xi}$ are the MLEs of λ,γ and ξ under H_1 and $\tilde{\lambda}$ and $\tilde{\xi}$ are the MLEs of λ and ξ under H_0. Then, the corresponding p-value is given by p-value $= P(K \geq w)$, where K denotes a random variable following the χ_2 distribution with 1 degree of freedom.

4.2. Simulation study

This section proposes a Monte Carlo simulation survey to evaluate numerically the performance of the MLEs $\hat{\lambda}$, $\hat{\gamma}$ and $\hat{\theta}$ of the GOIE-E$(\lambda, \gamma, \theta)$ model parameters presented in Subsection 2.1. To achieve this purpose, we carried out a program R to generate $N = 650$ times samples of sizes $n = 55 + 5q$, with $q \in \{1, \ldots, 121\}$ from the qf of the GOIE-E distribution whose initial parameters are $\lambda = 2$, $\gamma = 1$ and $\theta = 1$ and from the uniform distribution. For each generated sample $i \in \{1, \ldots, N\}$, we calculate $(\hat{\lambda}_i, \hat{\gamma}_i, \hat{\theta}_i)$. Then, we estimate the following measures: bias, mean square error (MSE), average length (AL) and coverage probability (CP). For $\epsilon \in \{\lambda, \gamma, \theta\}$ and $i \in \{1, \ldots, N\}$, by denoting $\hat{\epsilon}_i$ the MLE of ϵ_i and $s_{\hat{\epsilon}_i}$ is the standard error of $\hat{\epsilon}_i$, they are respectively defined by

$$\widehat{Bias}_\epsilon(n) = \frac{1}{N}\sum_{i=1}^{N}(\hat{\epsilon}_i - \epsilon), \quad \widehat{MSE}_\epsilon(n) = \frac{1}{N}\sum_{i=1}^{N}(\hat{\epsilon}_i - \epsilon)^2, \quad \widehat{AL}_\epsilon(n) = \frac{3.919928}{N}\sum_{i=1}^{N} s_{\hat{\epsilon}_i}$$

and

$$\widehat{CP}_\epsilon(n) = \frac{1}{N}\sum_{i=1}^{N} I(\hat{\epsilon}_i - 1.95996 s_{\hat{\epsilon}_i}, \hat{\epsilon}_i + 1.95996 s_{\hat{\epsilon}_i}),$$

where $I(A)$ denotes the indicator function over a set A.

These statistical quantities enable to measure the precision of the MLE $\hat{\epsilon}$. After compilation of our R code, we obtain the plots of them shown in Figures 9 to 12. From Figure 9 and Figure 10, we remark that, when $n \to \infty$, biases and MSEs tend towards zero, respectively. This reveals the MLEs are asymptotically unbiased and consistent. We see in Figure 11 that ALs decrease when $n \to \infty$. In Figure 12, the CPs are near to 0.95 and approach to the nominal value when n increases. All these observations are consistent with the theoretical properties of the MLEs. Finally, let us mention that these numerical results still hold for other test values of λ, γ and θ.

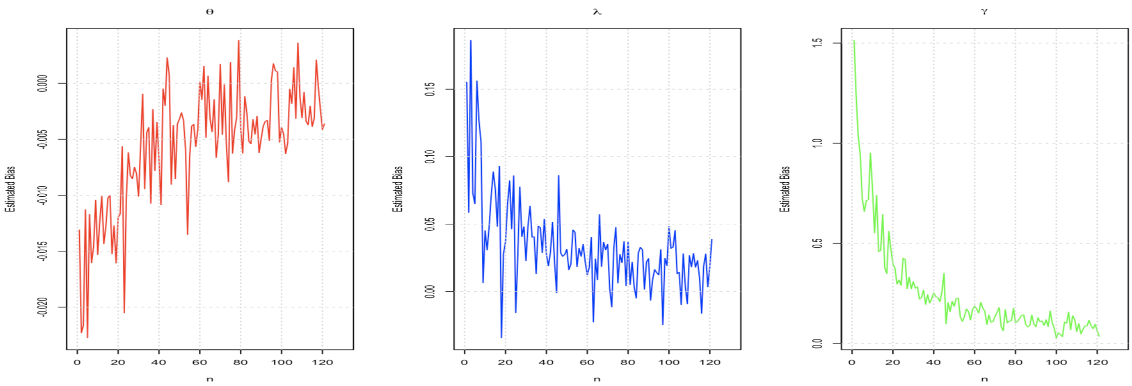

Figure 9: Plots of biases of λ, γ and θ.

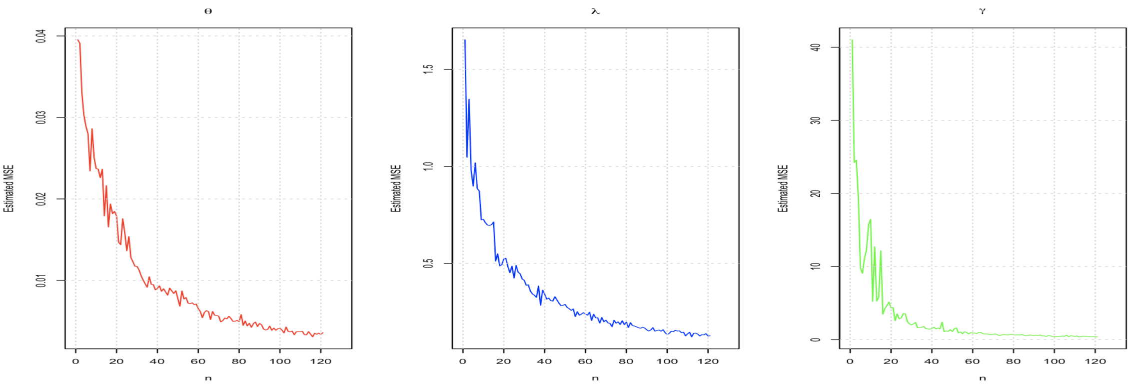

Figure 10: Plots of MSEs of λ, γ and θ.

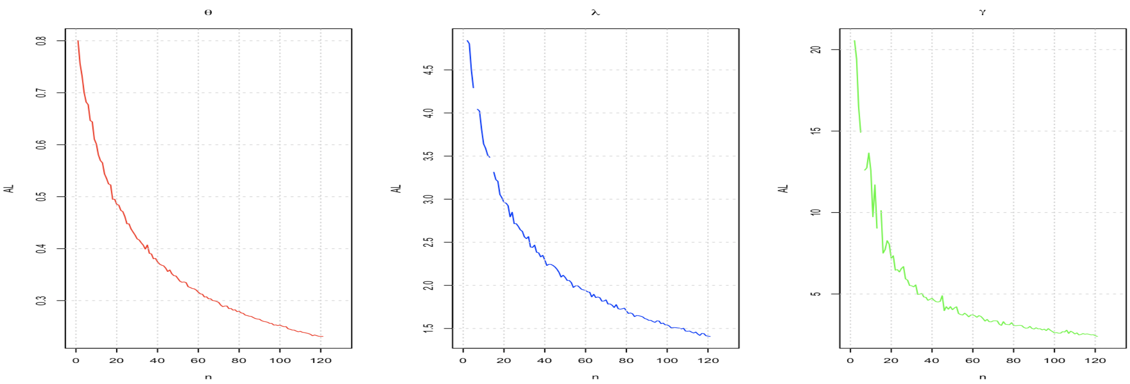

Figure 11: Plots of ALs of λ, γ and θ.

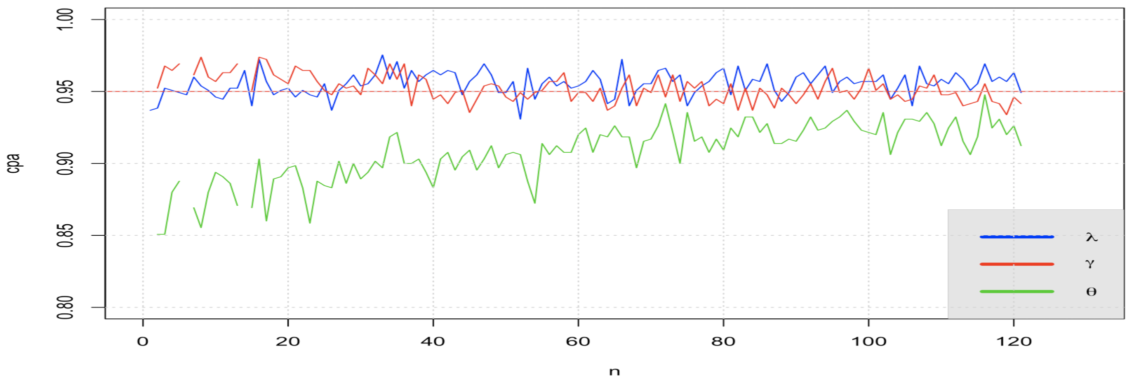

Figure 12: Plots of CPs of λ, γ and θ.

5. Applications

In this section, the potential of applicability of the GOIE-G family is demonstrated. We compare the fits of the GOIE-E, GOIE-L and GOIE-W models derived to the special distributions presented in Section 2 to other well-established models via three practical data sets. We perform R code using the goodness-of-fit function to compute each time the parameters of a fitted model. Firstly, we give a descriptive summary of each data set and provide the MLEs of the model parameters. Secondly, we adopt some standard goodness-of-fit statistics such that : the Cramer-Von Mises (W^*) and Anderson Darling (A^*) statistics described in [9], the Akaike Information Criterion (AIC), Bayesian Information Criterion (BIC) and Kolmogorov-Smirnov test (K-S) and its p-value and so on to compare the fitted models and check which models give a better to data set. When it is appropriate, we provide the LR test on the first data to prove the benefit of the parameter γ.

5.1. Fatigue time data

The first data set consists of the Fatigue time of 101 6061-T6 aluminum coupons cut parallel to the direction of rolling and oscillated at 18 cycles per second : 70, 90, 96, 97, 99, 100, 103, 104, 104, 105, 107, 108, 108, 108, 109, 109, 112, 112, 113, 114, 114, 114, 116, 119, 120, 120, 120, 121, 121, 123, 124, 124, 124, 124, 124, 128, 128, 129, 129, 130, 130, 131, 131, 131, 131, 131, 132, 132, 132, 133, 134, 134, 134, 134, 134, 136, 136, 137, 138, 138, 138, 139, 139, 141, 141, 142, 142, 142, 142, 142, 142, 144, 144, 145, 146, 148, 148, 149, 151, 151, 152, 155, 156, 157, 157, 157, 157, 158, 159, 162, 163, 163, 164, 166, 166, 168, 170, 174, 196, 212. These data can be found in [8] or [21], for instance.

Table 2 gives a summary descriptive statistics of this data set. Table 3 contains the estimated parameters of the GOIE-W, GOIE-L and GOIE-E models obtained after execution of the goodness-of-fit function. Table 4 features some statistics of goodness-of-fit results, namely AIC and BIC, of the challenger models. From the second to last line of that table grant the goodness-of-fit statistics of the GOIE-W model and the challenger models used in [21], i.e., the extended odd Fréchet Nadarajah-Haghighi (EOFNH), odd Fréchet Nadarajah-Haghighi (OFNH), extended odd Fréchet Weibull (EOFW) and odd Fréchet Weibull (OFW) models, where EOFNH is the best fitted model for fatigue time data. According to Table 4, it is clear that the GOIE-W model has the lowest values of the AIC and BIC among all fitted models. Then, we can conclude that the GOIE-W model is adequate fitted model for fatigue time data, more than its challengers. Table 5 provides the following measures: $-\hat{\ell}$, AIC, BIC, W^*, A^*, KS and p-value, for the previously introduced GOIE-G special models.

We performed the likelihood ratio test whose results are recorded in Table 6 to assess the importance of adding parameter γ. Since p-value < 0.001, the reject of $H_0 : \gamma \neq 0$ is highly significant **(***)**. Hence, the addition of γ is of importance, which validates the use of our extended odd transformation from a statistical point of view.

Table 2: Descriptive statistics of the fatigue time data.

Mean	Median	SD	Variance	Skewness	Kurtosis	Min	Max
133.77	133.5	22.46517	504.6839	0.3240165	4.012784	70.0	212.0

Table 3: MLEs of the parameters.

Model	Estimate parameters			
GOIE-W(λ, γ, a, b)	**1.401807**	**4.526372**	**2.823993**	**97.068479**
GOIE-L(λ, γ, θ)	2.65708717	35.06728443	0.05309351	-
GOIE-E(λ, γ, θ)	14.04383305	18.69891849	0.04577799	-

Table 4: The AIC and BIC of the considered models.

Model	AIC	BIC
GOIE-W(λ, γ, a, b)	**911.7021**	**922.1228**
EOFNH(α, β, λ, θ)	948.7255	959.1860
OFNH(α, λ, θ)	953.1958	961.0412
EOFW(α, β, λ, θ)	950.5259	960.9864
OFW(α, λ, θ)	953.6325	961.4778

Table 5: The AIC, BIC, W^*, A^*, KS, and p-value of the considered GOIE-G models.

Model	Goodness of fit criteria						
	-$\hat{\ell}$	AIC	BIC	W^*	A^*	K-S	p-value
GOIE-W	**451.8511**	**911.7021**	**922.1228**	**0.04536376**	**0.2986486**	**0.05973**	**0.8678**
GOIE-L	457.2012	920.4024	928.2179	0.1704586	0.9619867	0.099801	0.2722
GOIE-E	458.3543	922.7087	930.5242	0.192183	1.087259	0.10419	0.2277

Table 6: LR test.

Hypothesis	w	p-value
$H_0 : \gamma = 0$ vs $H_1 : \gamma \neq 0$	13.43338	0.0002471858

We now propose to visually confirm the adequacy of the GOIE-W model to the fatigue time data. Through Figure 13, we see that the red curve, corresponding to the estimated pdf plot of the GOIE-W distribution, has the best fit of the histogram. The same is observed in Figure 14 with the estimated cdf plot of the GOIE-W distribution and the cumulative empirical distribution function. Figure 15 illustrates, in some sense, the small p-value of the GOIE-W model from the Kolmogorov-Smirnov test (see Table 5) by the fact that the scatter plot tends to merge with the pp-line. Finally, Figure 16 guarantees the uniqueness of the maxima of the corresponding log-likelihood function.

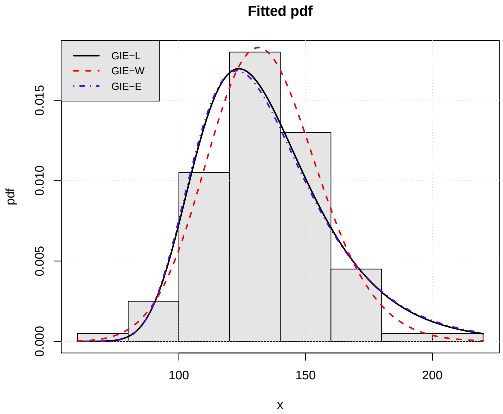

Figure 13: Plots of estimated pdfs.

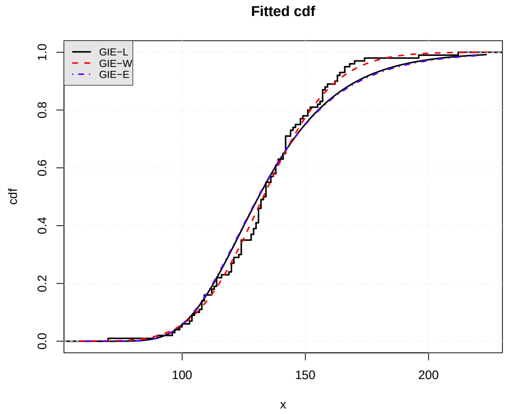

Figure 14: Plots of estimated cdfs.

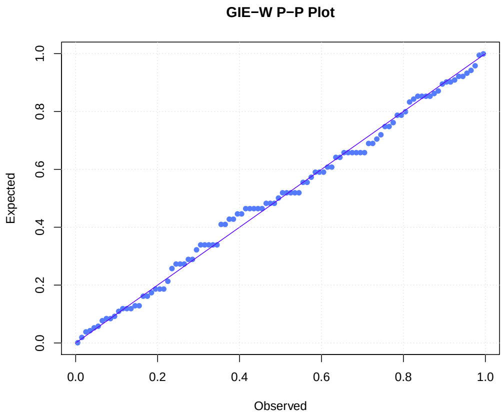

Figure 15: Plots of pp-plot.

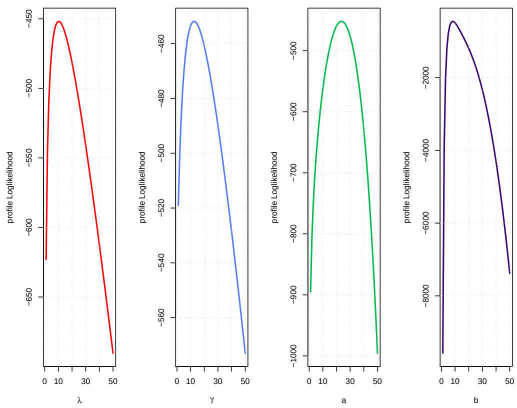

Figure 16: Plots of the log-likelihood function.

5.2. Glass fibers data

The second data set represents 63 observations of the strengths of 1.5 cm glass fibers, originally obtained by workers at the UK National Physical Laboratory : 0.55, 0.93, 1.25, 1.36, 1.49, 1.52, 1.58, 1.61, 1.64, 1.68, 1.73, 1.81, 2, 0.74, 1.04, 1.27, 1.39, 1.49, 1.53, 1.59, 1.61, 1.66, 1.68, 1.76, 1.82, 2.01, 0.77, 1.11, 1.28, 1.42, 1.5, 1.54, 1.6, 1.62, 1.66, 1.69, 1.76, 1.84, 2.24, 0.81, 1.13, 1.29, 1.48, 1.5, 1.55, 1.61, 1.62, 1.66, 1.7, 1.77, 1.84, 0.84, 1.24, 1.3, 1.48, 1.51, 1.55, 1.61, 1.63, 1.67, 1.7, 1.78, 1.89. It can be found in [16] and [22], for instance.

Table 7 provides a summary descriptive statistics of this data set. Table 8 contains the estimated parameters of the GOIE-W, GOIE-L and GOIE-E models. Table 9 features some statistics of goodness-of-fit results, namely AIC, BIC, W^* and A^* of the considered models. From the second to last line of that Table grant the goodness-of-fit statistics of the GOIE-W model and the challenger models used in [22], i.e., the transmuted generalized odd generalized exponential Exponential (TGOGE-E), Weibull Fréchet (WFr), Kumaraswamy Weibull (KwW) and Kumaraswamy Fréchet (KwF) models, where TGOGE-E is the best fitted model for the considered data. According to Table 9, the GOIE-W model has the lowest values of AIC, BIC and W^*, and the greatest value of A^*, among all fitted models. Then, the GOIE-W model is a perfect fitted model for these data.

Table 10 provides the following statistical indicators: -$\hat{\ell}$, AIC, BIC, W^*, A^*, KS and p-value, for the previously presented GOIE-G special models.

Table 7: Descriptive statistics of the glass fibers data.

Mean	Median	SD	Variance	Skewness	Kurtosis	Min	Max
1.507	1.590	0.3241257	0.1050575	-0.8999263	3.923761	0.550	2.240

Table 8: MLEs of the parameters.

Model	Estimate parameters			
GOIE-W(λ, γ, a, b)	**0.02275868**	**117.59832983**	**5.02582583**	**1.46907704**
GOIE-L(λ, γ, θ)	1.338556	20.882618	3.050187	-
GOIE-E(λ, γ, θ)	0.5442407	62.3584487	2.6590564	-

Table 9: The AIC, BIC, W^* and A^* of the considered models.

Model	AIC	BIC	W^*	A^*
GOIE-W(λ, γ, a, b)	**29.9825**	**38.55504**	**0.08205409**	**0.4750684**
TGOGE-E(α, β, λ, a)	39.000	47.573	1.3410	0.2326
WFr(a, b, α, β)	39.6622	48.2347	1.5006	0.2753
KwW(α, β, a, b)	40.7852	49.3577	1.59965	0.29207
KwFr(α, β, a, b)	42.3913	50.9638	1.7445	0.309542

Table 10: The AIC, BIC, W^*, A^*, KS, and p-value of the considered GOIE-G models.

Model	Goodness of fit criteria						
	$-\hat{\ell}$	AIC	BIC	W^*	A^*	KS	p-value
GOIE-W	**10.99125**	**29.9825**	**38.55504**	**0.08205409**	**0.4750684**	**0.097018**	**0.5935**
GOIE-L	29.74279	65.48558	71.91498	0.7291001	3.992747	0.22138	0.004161
GOIE-E	30.54727	67.09455	73.52395	0.7544446	4.126297	0.22399	0.003594

In Figures 17 and 18, we can see respectively, the good fit of the estimated pdf and cdf plot of the GOIE-W distribution to the histogram and the cumulative empirical distribution function of this data set. This is also illustrated in Figure 19 with a good adjustment of the pp-line. Finally, Figure 20 guarantees the uniqueness of the MLEs for the GOIE-W model parameters.

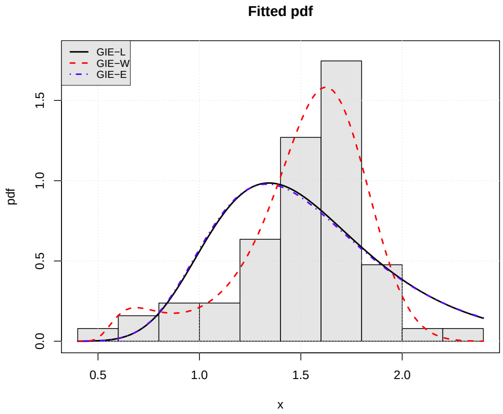

Figure 17: Plots of estimated pdfs.

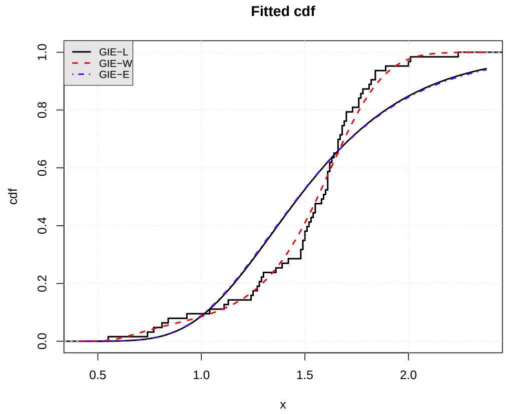

Figure 18: Plots of estimated cdfs.

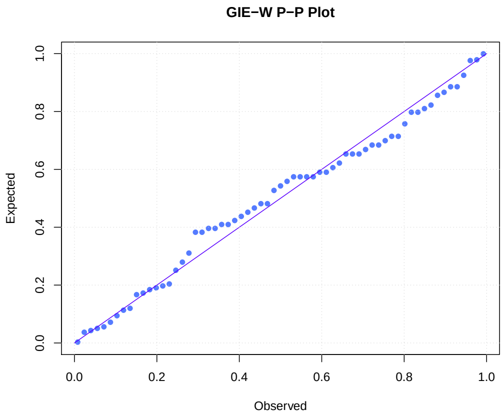

Figure 19: Plots of pp-plot.

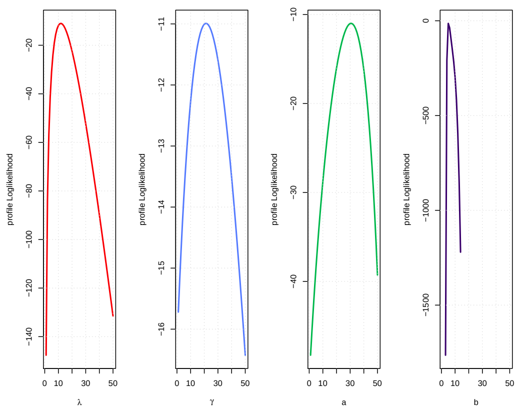

Figure 20: Plots of the log likelihood function.

5.3. Gauge length data

The following data can be found in [18] and [22]: 1.901, 2.132, 2.203, 2.228, 2.257, 2.350, 2.361, 2.396, 2.397, 2.445, 2.454, 2.474, 2.518, 2.522, 2.525, 2.532, 2.575, 2.614, 2.616, 2.618, 2.624, 2.659, 2.675, 2.738, 2.740, 2.856, 2.917, 2.928, 2.937, 2.937, 2.977, 2.996, 3.030, 3.125, 3.139, 3.145, 3.220, 3.223, 3.235, 3.243, 3.264, 3.272, 3.294, 3.332, 3.346, 3.377, 3.408, 3.435, 3.493, 3.501, 3.537, 3.554, 3.562, 3.628, 3.852, 3.871, 3.886, 3.971, 4.024, 4.027, 4.225, 4.395, 5.020. It corresponds to 63 observations of gauge length of 10 mm.

Table 11 provides a summary descriptive statistics of gauge length data. Table 12 contains the estimated parameters of the GOIE-W, GOIE-L and GOIE-E models. And Table 13 features some statistics of goodness-of-fit results, namely AIC, BIC, W^* and A^* of the challenger models. From the second to last line of this table grant the goodness-of-fit statistics of the GOIE-W model and the challenger models used in [22], i.e., the transmuted generalized odd generalized exponential Lomax (TGOGE-Lx), Weibull Lomax (WLx), transmuted Weibull Lomax (TWLx), modified Beta Weibull (MBW) and MacDonald Lomax (McLx) models, where TGOGE-Lx is the best fitted model for gauge length data. From this table, it is clear that GOIE-W distribution has the lowest values of AIC, BIC and W^*, and the greatest A^*, among all fitted models. Then, the GOIE-W model is ideal to fit the gauge length data. Table 14 provides the measures: -$\hat{\ell}$, AIC, BIC, W^*, A^*, KS and p-value of the GOIE-G special models previously introduced. We can see from Table 14 that the GOIE-W model is not the best model for the gauge length data in comparison to the GOIE-L and GOIE-E models for some criteria, but it remains better than its competitors as seen in Table 13.

Table 11: Descriptive statistics of gauge length data.

Mean	Median	SD	Variance	Skewness	Kurtosis	Min	Max
3.059	2.996	0.6209216	0.3855436	0.6328486	3.286345	1.901	5.020

Table 12: MLEs of the parameters.

Model	Estimate parameters			
GOIE-W(λ, γ, a, b)	**3.862337**	**12.511301**	**1.356270**	**1.010798**
GOIE-L(λ, γ, θ)	11.665026	11.527414	2.181696	-
GOIE-E(λ, γ, θ)	10.228128	20.685798	1.950573	-

Table 13: The AIC, BIC, W^* and A^* of the considered models.

Model	AIC	BIC	W^*	A^*
GOIE-W(λ, γ, a, b)	**120.6947**	**129.2672**	**0.06364581**	**0.3359475**
TGOGE-Lx(α, β, a, b, δ)	122.4580	133.1740	0.3256	0.0621
WLx(α, β, a, b)	129.7870	138.3595	0.8122	0.1174
TWLx(α, β, λ, a, b)	132.3841	143.0998	0.8339	0.1205
MBW(α, β, λ, a, b)	135.9170	142.4895	1.0436	0.1517
McLx(α, β, λ, a, b)	140.5970	147.1695	0.8142	0.1081

Table 14: The AIC, BIC, W^*, A^*, KS, and p-value of the considered GOIE-G models.

Model	Goodness of fit criteria						
	$-\hat{\ell}$	AIC	BIC	W^*	A^*	KS	p-value
GOIE-L	**56.45528**	**118.9106**	**125.34**	**0.06895279**	**0.3576401**	**0.087596**	**0.7191**
GOIE-E	56.51405	119.0281	125.4575	0.07068436	0.3662847	0.08877	0.7036
GOIE-W	56.34733	120.6947	129.2672	0.06364581	0.3359475	0.083025	0.778

Figures 21 and 22 visually confirm the adequacy of the GOIE-W model to the gauge length data via the plots of the estimated pdf and cdf. Figure 23 proves that the pp-line well-adjusted the scatter plot, confirming the good fit of the model. Last but not least, Figure 24 shows the uniqueness of the MLEs for the GOIE-W model parameters.

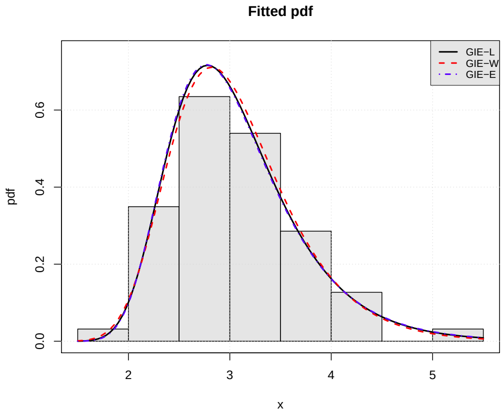

Figure 21: Plots of estimated pdfs.

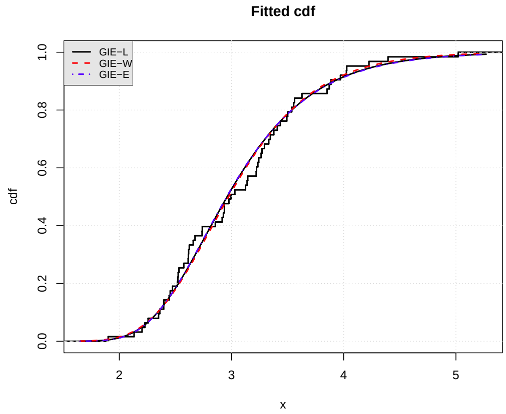

Figure 22: Plots of estimated cdfs.

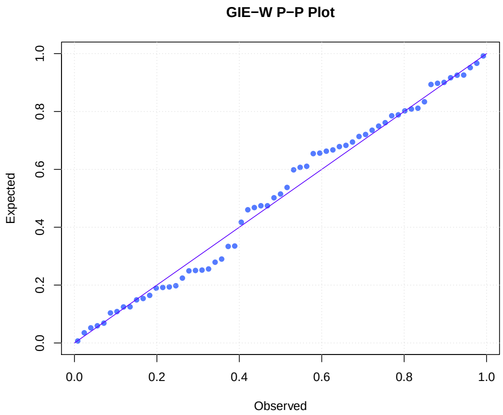

Figure 23: Plots of pp-plot.

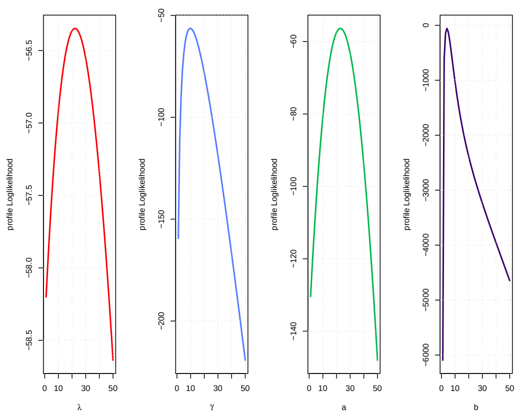

Figure 24: Plots of the log-likelihood function.

6. Conclusion

In this article, we propose a new class of continuous distribution called the generalized odd inverted exponential-G (GOIE-G) family. We introduce some of its mathematical properties such that the asymptotic, the quantile function, some linear representations, the moments, the reliability, the entropy, the order statistics and a bivariate extension. Then, the maximum likelihood estimation of the parameters is investigated and a Monte Carlo simulation is performed to assess the quality of the obtained estimates. In order to demonstrate the usefulness and flexibility of the GOIE-G family, we illustrate it through three practical data sets. Nice fits are obtained, challenging modern statistical models. As perspectives of future works, we can think to extend any generalized family of distributions defined with the standard odd transformation by using the proposed extending odd transformation instead, opening new perspectives of applications.

Acknowledgments: The authors would like to thank the referees for their thorough and constructive comments which helped to improve the manuscript.

References

[1] Alizadeh, M., Altun, E., Cordeiro, G. M. and Rasekhi, M. (2018). The odd power Cauchy family of distributions: properties, regression models and applications. Journal of Statistical Computation and Simulation, 88(4): 785-805.

[2] Alizadeh, M., Emadiz, M., Doostparast, M., Cordeiro, G. M., Ortega, E. M. M. and Pescim, R. R. (2015). A new family of distributions : the Kumaraswamy odd log-logistic, properties and applications. Hacettepe Journal of Mathematics and Statistics, 44: 1491-1512.

[3] Alrajhi, S. (2019). The odd Fréchet inverse exponential distribution with application. Journal of Nonlinear Sciences and Applications, 12(8): 535-542.

[4] Alzaatreh, A., Famoye, F. and Lee, C. (2014). The gamma-normal distribution: Properties and applications. Computational Statistics and Data Analysis, 69: 67-80.

[5] Alzaatreh, A., Famoye, F. and Lee, C. (2013). A new method for generating families of continuous distributions. METRON, 71(1): 63-79.

[6] Alzaghal, A., Famoye, F. and Lee, C. (2013). Exponentiated T-X family of distributions with some applications. International Journal of Statistics and Probability, 2: 31-49.

[7] Amini, M., MirMostafaee, S. M. T. K. and Ahmadi, J. (2014). Log-gamma-generated families of distributions. Statistics, 48(4): 913-932.

[8] Birnbaum, Z. W. and Saunders, S. C. (1969). Estimation for a family of life distribution with applications to fatigue times. Journal of Applied Probability, 6(2): 328-347.

[9] Chen, G. and Balakrishnan, N. (1995). A general purpose approximate goodness-of-fit test. Journal of Quality Technology, 27(2): 154-161.

[10] Chen, G., Bunce, C. and Jiang, W. (2010). A new distribution for extreme value analysis. In: Proceedings of the International Conference on Computational Intelligence and Software Engineering, 1-4.

[11] Cordeiro, G. M., Alizadeh, M. and Ozel, G. (2017). The generalized odd log-logistic family of distributions: properties, regression models and applications. Journal of Statistical Computation and Simulation, 87(5): 908-932.

[12] Cordeiro, G. M., Ortega, E. M. M. and da Cunha, D. C. C. (2013). The exponentiated generalized class of distributions. Journal of Data Science, 11: 1-27.

[13] Eugene, N., Lee, C. and Famoye, F. (2002). Beta-normal distribution and its applications. Communications in Statistics-Theory and Methods, 31(4): 497-512.

[14] Galton, F. (1883). Inquiries into human faculty and its development. Macmillan and Company. London, Macmillan.

[15] Haq, M. A. and Elgarhy, M. (2018). The odd Fréchet-G family of probability distributions. Journal of Statistics Applications and Probability, 7(1): 189-203.

[16] Haq, M. A., Yousof, H. M. and Hashmi, S. (2017). A New five-parameter Fréchet model for extreme values. Pakistan Journal of Statistics and Operation Research, 13(3): 617-632.

[17] Kotz, S., Lumelskii, Y. and Penskey, M. (2003). The stress-strength model and its generalizations and applications. World Scientific, Singapore.

[18] Kundu, D., and Raqab, M. Z. (2009). Estimation of $R = P(Y < X)$ for three-parameter Weibull distribution. Statistics and Probability Letters, 79(17): 1839-1846.

[19] Moors, J. J. A. (1988). A quantile alternative for Kurtosis. Journal of the Royal Statistical Society, Series D (The Statistician), 37(1): 25-32.

[20] Murthy, D. P., Xie, M. and Jiang, R. (2004). Weibull models. John Wiley and Sons, Vol. 505.

[21] Nasiru, S. (2018). Extended odd Fréchet-G family of distributions. Journal of Probability and Statistics, 2018, (1): 1-12.

[22] Reyad, H., Othman, S. and Haq, M. A. (2019). The transmuted generalized odd generalized exponential-G family of distribution: Theory and application. Journal of Data Science, 17(2): 279-300.

[23] Ristić, M. M. and Balakrishnan, N. (2012). The gamma-exponentiated exponential distribution. Journal of Statistical Computation and Simulation, 82(8): 1191-1206.

[24] Torabi, H. and Montazari, N. H. (2012). The gamma-uniform distribution and its applications. Kybernetika, 48(1): 16-30.

[25] Torabi, H. and Montazari, N. H. (2014). The logistic-uniform distribution and its applications. Communications in Statistics-Simulation and Computation 43(10), 2551-2569.

[26] Zografos, K. and Balakrishnan, N. (2009). On families of beta- and generalized gamma-generated distributions and associated inference. Statistical Methodology, 6(4): 344-362.